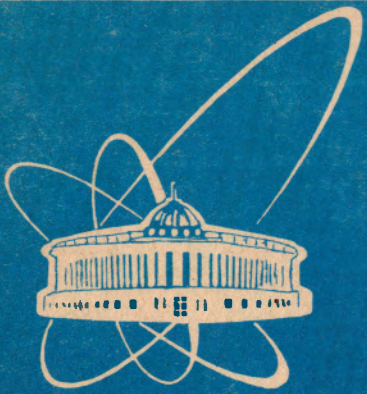

ОБЪЕДИНЕННЫЙ
ИНСТИТУТ
ЯДЕРНЫХ
ИССЛЕДОВАНИЙ

Дубна

E2-96-304

M.V.Tokarev

SPIN-DEPENDENT PARTON DISTRIBUTIONS FROM DEEP-INELASTIC SCATTERING

Talk presented at International Symposium on High-Energy Spin Physics «SPIN'96», 10—14 September, 1996, Amsterdam, The Netherlands

1996

Токарев М.В.
E2-96-304

Спин-зависимые партонные распределения
из глубоконеупругого рассеяния

Рассматривается феноменологическая процедура построения спин-зависимых партонных распределений. Предположения о знаках распределений морских кварков мотивированы механизмом 't Hooft для кварк-кваркового взаимодействия, индуцированного инстантонами. Партонные распределения Δu_V, Δd_V, $\Delta\bar{u}$, $\Delta\bar{d}$, Δs, ΔG построены с учетом аксиальной глюонной аномалии и данных о вкладе кварков Δu, Δd, Δs в спин протона. Исследовалась возможность положительного и отрицательного знака у глюонного распределения ΔG. Проведены расчеты структурных функций g_1^p, g_1^D, g_1^n и сравнение результатов с экспериментальными данными.

Работа выполнена в Лаборатории высоких энергий ОИЯИ.

Препринт Объединенного института ядерных исследований. Дубна, 1996

Tokarev M.V.
E2-96-304

Spin-Dependent Parton Distributions
from Deep-Inelastic Scattering

The phenomenological procedure to construct spin-dependent parton distributions is considered. It is based on some assumptions on signs of sea parton distributions motivated by t'Hooft mechanism of the quark-quark interaction induced by instantons. The spin-dependent parton distributions Δu_V, Δd_V, $\Delta\bar{u}$, $\Delta\bar{d}$, Δs, ΔG taking into account the axial gluon anomaly and the data on quark contributions Δu, Δd, Δs to the proton spin are constructed. The possibility of positive and negative sign of ΔG is studied. The obtained results of x- and Q^2-dependences of structure fucntions g_1^p, g_1^D, g_1^n are compared with experimental data.

The investigation has been performed at the Laboratory of High Energies, JINR.

Preprint of the Joint Institute for Nuclear Research. Dubna, 1996

1 Introduction

The new data on deep inelastic spin-dependent proton g_1^p and deuteron g_1^D structure functions from SLAC [1, 2] and CERN [3] stimulate exiting interest to determine spin-dependent quark and especially gluon distributions and quark contributions to the proton spin. The decision of the problem is out of the pQCD. Therefore numerous parametrizations both spin-independent and spin-dependent parton distributions are constructed and used for the analysis of experimental data. As the parton distributions are of universal nature the parametrizations can be used for simulation not only processes of deep-inelastic scattering but, in particularly, $p-p$ interaction with polarized proton beams for future research programs at colliders RHIC, LHC and HERA.

The direct information on parton distributions are extracted from the deep-inelastic lepton-proton and lepton-deuteron scattering. The measurable observables are asymmetries A^p, A^D. The structure function g_1^p can be expressed via A^p as follows

$$g_1^p(x,Q^2) = A^p(x,Q^2) \cdot \frac{F_2^p(x,Q^2)}{2x(1+R(x,Q^2)}. \qquad (1)$$

The additional information on the structure function F_2^p and the ratio of longitudinal to transverse photon cross section $R(x,Q^2) = \sigma_L/\sigma_T$ are necessary [4] to determine g_1^p. The similar formula takes place for the deuteron structure function.

The extraction of the parton distributions from the experimental data (g_1^p, g_1^D) of deep inelastic scattering is not direct and therefore it is very important to develop flexible procedures to construct the distributions taking into account features of experimental data and theoretical constraints of proton model.

At present time there are not strong arguments on the sign of the spin-dependent gluon distribution ΔG therefore one can suppose that the sign of ΔG may be both positive and negative [5]. Therefore we shall consider both possibilities in the paper. It is very important from experimental point of view to find the observables which are sensitive to sign of ΔG. As we shall show later the neutron structure function g_1^n can be one of such observables.

The spin-dependent parton distributions were constructed, in particular, in [6, 7, 10].

The Drell-Yan inclusive-exclusive connection relating the high Q^2-behaviour of hadron form-factors and the large x-limit of the quark distributions was used in [6]

$$F(Q^2) \longrightarrow \frac{1}{(Q^2)^n},\ at\ Q^2 \to \infty \Leftrightarrow G_{q/p} \longrightarrow (1-x)^{2n-1+2\Delta S},\ at\ x \to 1, \qquad (2)$$

where $\Delta S = 0, 1$ for the parallel and anti-parallel quark and photon helicity, respectively. Authors emphasized that this counting rule reflects the fact that the valence Fock state with minimal number of constituents gives the leading contribution to the structure function when one quark carries nearly all of the light cone momentum. The helicity dependence of the rule reflects the helicity retention property of the gauge couplings: a quark with a large momentum fraction of the hadron also tends to carry its helicity. The anti-parallel helicity quark is suppresed by the relative factor $(1-x)^2$. The obtained spin-dependent quark and gluon distributions were used to calculate the proton, neutron and deuteron structure functions and to compare with experimental data.

The LO QCD fit of EMC, SMC and SLAC data for g_1^N was performed in [7]. Polarized parton distributions were constructed by using two scenario - "standard" and "valence"

one. First scenario assumed that the neutron and hyperon β-decay data fix the total helicity both of valence and sea quarks $\Delta u+\Delta\bar{u}-\Delta d-\Delta\bar{d}=F+D$ and $\Delta u+\Delta\bar{u}+\Delta d+\Delta\bar{d}-2(\Delta s+\Delta\bar{s})=3F+D$, second one - only of the valence quarks $\Delta u_V-\Delta d_V=F+D$ and $\Delta u_V+\Delta d_V=3F+D$. In the "standard" scenario it was needed $\Delta s<0$ in order to obtain agreement with experiment data. In the "valence" scenario $\Delta\bar{q}<0$ even for the maximally $SU_f(3)$ broken polarized sea $\Delta s=\Delta\bar{s}=0$. It was found that results for Γ_1^p and Γ_1^n were in satisfactory agreement with SMC [12, 14] and E143 [2] data for both scenario.

The global LO fit to proton data on g_1^p to extract spin-dependent parton distributions was performed in [8]. It was assumed that the intrinsic polarization of strange quark was no significant. Non-zero polarization SU(3) symmetric sea quark distributions were generated dynamically at higher Q^2 by the evolution of the singlet distribution $\Delta\Sigma$. It was found that $\Delta\bar{q}$ was sensitive to the initial shape of the gluon distribution and therefore the measurement of polarization of sea quark distributions was proposed. The shape of the parton distributions was used as follows

$$x\Delta q_f\sim x^{\alpha_f}(1-x)^{\beta_f}(1+\gamma_f x). \tag{3}$$

Additional theoretical constraints at large and small x based on dimensional counting and Regge behaviour arguments were supposed. The different choices of γ_f correspond to different fits of ΔG at $x\to 1$: $G\uparrow\sim G\downarrow$, $G\uparrow\gg G\downarrow$, $G\uparrow\ll G\downarrow$ were studied. It was found that quark distributions were almost independent of the gluon distribution and the parameter α_f had the value close to the corresponding unpolarise one [9].

The detailed NLO QCD analysis of the proton and deuteron data on g_1 were performed in [10]. The singlet $\Delta\Sigma$, nonsinglet Δq_{NS} and gluon ΔG distributions were determined. The parton distributions were parametrized according to

$$\Delta q_f(x,Q_0^2)=N(\alpha_f,\beta_f,a_f)\eta_f x^{\alpha_f}(1-x)^{\beta_f}(1+a_f x), \tag{4}$$

where $N(\alpha_f,\beta_f,a_f)$ is the normalization coefficient. The various parameters in (4) were found by fitting $g_1(x,Q^2)$ to proton and deuteron experimental data. The data constrain the size of polarized parton distributions. It was emphasized that the main NLO effect is the direct gluon contribution to the first moment of g_1 and effects which are formally next-to leading order may lead to significant evolution because of the large contribution of polarized gluons to g_1 driven by the axial anomaly. The size of the gluon distribution drives perturbative evolution and due to the fact that the SMC and E143 data were obtained at the different value of Q^2 turns out to require the parameter η_g and consequently the polarized gluon distribution to be large and positive.

In present paper the phenomenological method to construct spin-dependent parton distributions is developed. Some constraints (a shape and sign of distributions) on parton distribution are used. The method takes into account the effect of axial anomaly to include under consideration the gluon distribution ΔG. The possibility of the positive and negative sign of the gluon distribution is studied. The new spin-dependent parton distributions are constructed. The dependence of Δq_f and structure functions g_1^p, g_1^n and g_1^D on x and Q^2 are investigated and the obtained results are compared with experimental data.

2 Method

The spin-dependent proton g_1^p structure function is expressed via spin-dependent parton distributions as follows

$$g_1^p(x,Q^2)=\frac{1}{2}\cdot\{\frac{4}{9}\Delta u+\frac{1}{9}\Delta d+\frac{1}{9}\Delta s\}, \tag{5}$$

where $\Delta q_f=q_f^+-q_f^-$ and $q_f^\pm$ are probability distributions to find the quark with the positive $(+)$ and negative $(-)$ helicity relatively to positive proton one. The neutron $g_1^n(x,Q^2)$ structure function can be written in the similar form by the replacement $\Delta u\leftrightarrow\Delta d$. The valence distributions $\Delta u_V,\Delta d_V$ are expressed as follows $\Delta u_V=\Delta u-2\Delta\bar{u}$. In the paper we shall construct the spin-dependent parton distributions. Let us now shortly describe the main items of the method used.

2.1 Shape of parton distributions

The form of the spin-dependent parton distribution Δq_f is taken as

$$\Delta q_f=sign(q_f)\cdot x^{\alpha_f}\cdot(1-x)^{\beta_f}\cdot q_f,\quad q_f=u_V,d_V,\bar{u},\bar{d},s,G \tag{6}$$

Here q_f is the spin-independent parton distribution, α_f,β_f are free parameters which should be found from the comparison with experimental data. We would like to note that there is the additional restriction for Δq_f

$$|\Delta q_f|<q_f. \tag{7}$$

It means that both the distributions q_f^+, q_f^- and $q_f=q_f^++q_f^-$ are to be positive. According to the equation the parameter β_f should be not negative. However if q_f is not connected with the parton distribution the parameter can be chosen as negative one. In this case the form of the spin-dependent parton distribution can be rewritten as

$$\Delta q_f=sign(q_f)\cdot x^{\alpha_f}\cdot q_f^R. \tag{8}$$

The equation (7) is satisfied and $q_f^R=(1-x)^{\beta_f}\cdot q_f$ can be considered as the renormalised parton distribution.

We would like to emphasize that numerous procedures to construct both spin - independent and spin - dependent distributions are ambiguously and therefore the restrictions on Δq_f can give the additional constraints on spin-independent distributions and develop flexible scheme to construct helicity parton distributions q_f^+ and q_f^-, separately.

2.2 Signs of parton distributions

We shall suppose that the sign of ΔG may be both positive and negative in the framework of our model-dependent investigation of the sign of ΔG because at present time there are no experiments to measure the ΔG directly.

For valence quarks distributions the situation is more definite. Therefore the signs of Δu_V and Δd_V are considered to be positive and negative, respectively. The choice is argued that the dominant configuration in the proton wave function is $u(\uparrow)u(\uparrow)d(\downarrow)$ (the arrow denotes the quark spin direction). Numerous analyses of experimental data on quark contributions to proton spin also confirm the choice [1, 2, 3], [11]-[14].

We shall suppose that the positive sign of $\Delta\bar{u}$ and negative one of $\Delta\bar{d}$, for the spin configuration $u(\uparrow)u(\uparrow)d(\downarrow)$ of proton wave function are motivated by 't Hooft mechanism [16]. The mechanism determines the dynamics of quark helicity flips. The incoming left helicity quark $q_L = (1+\gamma_5)q/2$ scattered from a zero modes in the instanton field is to be outgoing right helicity quark $q_R = (1-\gamma_5)q/2$. Effective Lagrangians were constructed in [17]. In the particular case $N_f = 2$ flavour it can be presented as follows:

$$L = \int d\rho \cdot n(\rho)(\frac{4}{3}\pi^2\rho^3)^2\{\bar{u}_R u_L \bar{d}_R d_L[1 + \frac{3}{32}(1 - \frac{3}{4}\sigma^u_{\mu\nu}\sigma^d_{\mu\nu})\lambda^a_u\lambda^a_d] + (R \leftrightarrow L)\}. \quad (9)$$

Here ρ is the size of instanton, $n(\rho)$ is the instanton density, $\sigma_{\mu\nu} = i/4 \cdot (\gamma_\mu\gamma_\nu - \gamma_\nu\gamma_\mu)$, λ^a are the matrices for $SU_c(3)$ group. If the left helicity quark scatters off instanton, then it becomes right helicity one and $q_R\bar{q}_R$ pair is created. The helicity of sea quarks is opposite to the initial quark. Therefore the spin flips of the valence quarks u^+ and d^- determine the signs of the sea quark distributions - negative for $\bar{d}$ and positive for $\bar{u}$. The negative sign of Δs is in agreement with the arguments mentioned above and is supported by the results of analysis of the determination of quark content to proton spin from the experimental data on g_1^p [1, 2, 3], [11]-[14].

2.3 Axial anomaly

It was shown in [18] that the flavour-singlet axial current

$$A^0_\mu = \sum_{f=u,d,s} \bar{q}_f\gamma_\mu\gamma_5 q_f \quad (10)$$

diverges at the quark level due to the one-loop triangle anomaly

$$\partial^\mu A_\mu = \frac{\alpha_s}{\pi} \cdot N_f \cdot tr\{F_{\mu\nu}\tilde{F}^{\mu\nu}\}, \quad (11)$$

where $\tilde{F}_{\mu\nu} = \epsilon_{\mu\nu\beta\gamma}F^{\beta\gamma}$, $F_{\mu\nu} = \partial_\mu A_\nu - \partial_\nu A_\mu + [A_\mu A_\nu]$, $A_\mu = A^a_\mu \cdot \lambda^a$, α_s is a coupling constant, N_f is number of flavours. The anomaly induced a mixing between gluon and the flavour singlet axial current of quarks. For this reason, the helicity carries by each flavour undergo renormalization

$$\Delta\tilde{q}_f(x,Q^2) = \Delta q_f - \frac{\alpha_s}{2\pi} \cdot \Delta G(x,Q^2). \quad (12)$$

It was suggested in [18] that the axial anomaly might play a key role, which would modify the naive quark model predictions and makes parton distributions more sensitive to sign of gluon distribution. So the axial anomaly allows one to include the ΔG under consideration structure functions g_1^p, g_1^n.

Note that the direct measurement of ΔG is possible in the experiments with polarized proton beams. That is why the measure of the asymmetry of direct photon production is planned in future polarization program at RHIC, LHC and HERA.

2.4 Relative parton contributions to proton spin

The results of analysis [19] of SMC and SLAC data on the structure functions g_1^p and g_1^D and Bjorken sum rule with pQCD corrections up to $O((\alpha_s/\pi)^3)$ for singlet combination have shown that the relative quark contributions to proton spin were $\Delta u = 0.83 \pm 0.03, \Delta d = -0.43 \pm 0.03, \Delta s = -0.10 \pm 0.03$ at a renormalization scale $Q_0^2 = 10\ (GeV/c)^2$. We shall use the values of the contributions and equation

$$\int_0^1 \Delta\tilde{q}_f(x,Q_0^2)dx = \Delta f, \quad f = u,d,s \quad (13)$$

to determine the free parameters α_f, β_f for spin-dependent parton distributions Δu_V, Δd_V, $\Delta\bar{u}$, $\Delta\bar{d}$, Δs, ΔG.

3 Results and Discussion

Tables 1-6 present the results for coefficients α_f, β_f obtained by the procedure described above. The unpolarized parton distributions q_f are taken from [20].

Figure 1(a,b) and 2(a,b) show the dependence of g_1^p and g_1^n on x for parametrizations of parton distribution constructed with positive (a) and negative (b) ΔG. The dashed, solid and dotted lines correspond to the parameters α_f, β_f taken from Tables 1-3 and 4-6, respectively.

Figure 1(a,b) shows that all theoretical curves g_1^p are in reasonable agreement with experimental data [1, 11, 14].

Figure 2(a,b) shows the qualitative difference for xg_1^n in the range $0.1 < x < 0.3$ between curves with positive and negative ΔG.

Figure 3(a,b) shows the x-dependence of $xg_1^p(x,Q^2)$ for $Q^2 = 1, 10, 100\ (GeV/c)^2$. The behaviour of $xg_1^p(x,Q^2)$ is qualitatively different for positive and negative ΔG. In the first case the maximum of the curve displaces to the low x with increasing Q^2, in the second one the maximum practically does not displace. For $x < 0.01$ the curve for $\Delta G > 0$ with $Q^2 = 1.0\ (GeV/c)^2$ lies lower than the curve with $Q^2 = 10\ (GeV/c)^2$. The curve for $\Delta G < 0$ with $Q^2 = 1.0\ (GeV/c)^2$ lies upper than the curve with $Q^2 = 10\ (GeV/c)^2$ in the range $10^{-3} < x < 1$.

Figure 4(a,b) shows the x-dependence of $xg_1^n(x,Q^2)$ at $Q^2 = 1, 10\ (GeV/c)^2$. The strong Q^2-dependence for $\Delta G < 0$ for $x < 0.1$ and the deep at $x \simeq 0.1 - 0.2$ are observed.

Figure 5(a,b) shows the x-dependence of the deuteron structure function $xg_1^D(x,Q^2)$ at $Q^2 = 1, 10, 100\ (GeV/c)^2$ and experimental data [2, 3, 12]. The dependences of $xg_1^D(x,Q^2)$ on Q^2 for $\Delta G > 0$ and $\Delta G < 0$ are qualitatively different from each other and similar to the proton ones.

Figure 6 shows the x-dependence of $xg_1^n(x,Q^2)$ for $Q^2 = 1, 3, 5, 10\ (GeV/c)^2$ and experimental data. The behaviour of $xg_1^n(x,Q^2)$ is qualitatively and quantitatively different for $\Delta G > 0$ and $\Delta G < 0$, especially for low Q^2. In the range $x < 0.1$ the experimental data on g_1^n for $Q^2 < 10\ (GeV/c)^2$ can be used to discriminate the parton distributions with different sign of ΔG.

The χ^2 criterium may be used as a quantitative characteristic to compare the theoretical results for xg_1^n with experimental data [2, 3, 13]. The obtained results are presented in Table 7. The references for experimental data on g_1^n, the values for average Q^2 and the number of experimental points are shown in column 1, 2 and 3, respectively. The mark 'all' denotes that the data are taken for different Q^2 and the value of χ^2 takes into account the Q^2-dependence of spin-dependent parton distributions. The value of Q^2 changes in the kinematic ranges $1.1 - 5.2\ (GeV/c)^2$ and $1.3 - 48.7\ (GeV/c)^2$ for E142 and SMC experiments, respectively. One can see from Table 7 that the χ^2 for $\Delta G > 0$ is smaller

than for $\Delta G < 0$ for all group of data. The choice of the parton parametrizations with positive ΔG is even more preferable when 'all' Q^2 data are used.

Tables 1-6. The parameters α_f, β_f and signs of spin-dependent parton distributions $\Delta q_f = sign(q_f) \cdot x^{\alpha_f} \cdot (1-x)^{\beta_f} \cdot q_f$ for positive and negative ΔG. The quark contributions to proton spin is denoted by I_f

Table 1

f	sign	α_f	β_f	I_f
ΔG	+	0.62790	0.000	
Δu_V	+	0.43763	−0.450	0.83
$\Delta \bar{u}$	+	0.54637	0.000	
Δd_V	−	0.71597	−0.450	−0.43
$\Delta \bar{d}$	−	0.57590	0.000	
Δs	−	0.96418	0.000	−0.1

Table 2

f	sign	α_f	β_f	I_f
ΔG	+	0.62790	0.000	
Δu_V	+	0.43763	−0.450	0.83
$\Delta \bar{u}$	+	0.54637	0.000	
Δd_V	−	0.71597	−0.450	−0.43
$\Delta \bar{d}$	−	0.57590	0.000	
Δs	−	0.96418	0.000	−0.1

Table 3

f	sign	α_f	β_f	I_f
ΔG	+	0.62076	0.000	
Δu_V	+	0.50424	−0.500	0.83
$\Delta \bar{u}$	+	0.46710	0.000	
Δd_V	−	0.70556	−0.500	−0.43
$\Delta \bar{d}$	−	0.58863	0.000	
Δs	−	1.00280	0.000	−0.1

Table 4

f	sign	α_f	β_f	I_f
ΔG	−	0.45000	0.000	
Δu_V	+	0.60176	−0.900	0.83
$\Delta \bar{u}$	+	1.0780	0.000	
Δd_V	−	0.34310	−0.900	−0.43
$\Delta \bar{d}$	−	0.56901	0.000	
Δs	−	0.31036	0.000	−0.1

Table 5

f	sign	α_f	β_f	I_f
ΔG	−	0.50000	0.000	
Δu_V	+	0.57443	−0.900	0.83
$\Delta \bar{u}$	+	1.0088	0.000	
Δd_V	−	0.54871	−0.900	−0.43
$\Delta \bar{d}$	−	0.45256	0.000	
Δs	−	0.34023	0.000	−0.1

Table 6

f	sign	α_f	β_f	I_f
ΔG	−	0.60000	0.000	
Δu_V	+	0.53379	−0.900	0.83
$\Delta \bar{u}$	+	0.98175	0.000	
Δd_V	−	0.53722	−0.900	−0.43
$\Delta \bar{d}$	−	0.50235	0.000	
Δs	−	0.39092	0.000	−0.1

The χ^2 for positive and negative ΔG are equal to 11.6 and 18.4 for the E142 data [13] and 16.2 and 28.9 for the SMC data [3]. The results can be considered as a quantitative evidence that the case with $\Delta G > 0$ is more preferable than $\Delta G < 0$ one.

We would like to note that our result supports the conclusion of positive sign of ΔG based on the NLO QCD fit of proton and deuteron data on g_1 made in [10]

Table 7. The value of χ^2 comptuted for $g_1^n(x, Q^2)$ for two choices of the parton distributions with the parameters α_f, β_f taken from Tables 2 and 5

Experiment	Q^2 $(GeV/c)^2$	data points	$\Delta G > 0$	$\Delta G < 0$
E142 [13]	2	8	9.56	16.4
E143 [2]	3	9	8.02	12.7
SMC [3]	10	12	15.4	19.5
HERMES [15]	3	8	6.87	9.56
E142 [13]	all	8	11.6	18.4
SMC [3]	all	12	16.2	28.9

Figures 7-9 and 10-12 show the dependences of the parton distributions Δu_V, Δd_V, $\Delta \bar{u}$, $\Delta \bar{d}$, Δs and ΔG on x and Q^2 for positive and negative ΔG, respectively. As one can see from Figures 7 and 10 the distributions of the valence quarks Δu_V and Δd_V for $\Delta G > 0$ and $\Delta G < 0$ are qualitatively similar to each other. The distributions for negative ΔG are larger than those for positive ΔG.

Figures 8(b,d) and 11(b,d) show that the sea distribution $x\Delta\bar{u}$ for $\Delta G > 0$ is larger than that for $\Delta G < 0$ in contrast to the $x\Delta\bar{d}$ distribution.

We would like to note that the signs for $x\Delta\bar{u}$ and $x\Delta\bar{d}$ are different from each other. The symmetry violation of the equation $\Delta\bar{u} = \Delta\bar{d}$ for negative ΔG is more stronger than for positive ΔG.

Figures 9(a,b) and 12(a,b) show the x- and Q^2-dependences of distributions for strange quark $x\Delta s$. The value of $x\Delta s$ for positive ΔG is less than 0.008 for $Q^2 = 5{-}1600\ (GeV/c)^2$ in the range $x = 10^{-3} - 1$. The distribution $x\Delta s$ for negative ΔG grows up to -0.05 at $x \simeq 10^{-3}$ for $Q^2 = 5, 10\ (GeV/c)^2$ and up to -0.15 for $Q^2 = 1600\ (GeV/c)^2$.

We would like to emphasize that the flavour violation for sea distributions $\Delta\bar{u}, \Delta\bar{d}$ and Δs for negative ΔG is more stronger than for positive one.

Figures 9(d) and 12(d) show that the "positive" gluon distribution $x\Delta G$ is five times less than "positive" one in the range $x = 10^{-3} - 1$ and $Q^2 = 10\ (GeV/c)^2$.

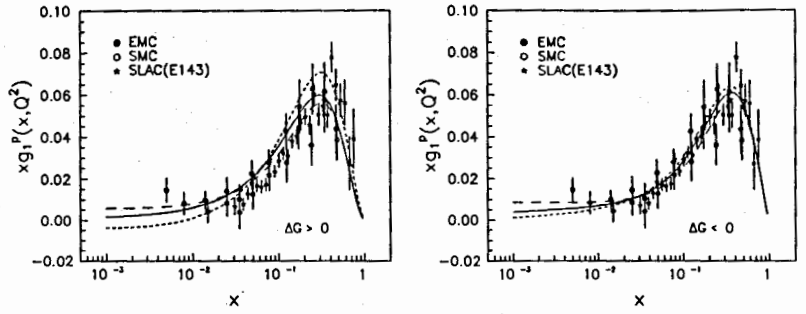

Figure 1. Deep-inelastic proton structure function $xg_1^p(x,Q^2)$. Experimental data: $\star$ - [1], $\bullet$ - [11], o - [14]. Theoretical curves: (a) - $\Delta G > 0$ and (b) - $\Delta G < 0$ at $Q^2 = 10\ (GeV/c)^2$ - - -, ——, — — are obtained with parameters α_f, β_f of parton distributions taken from Tables (1,4), (2,5) and (3,6), respectively.

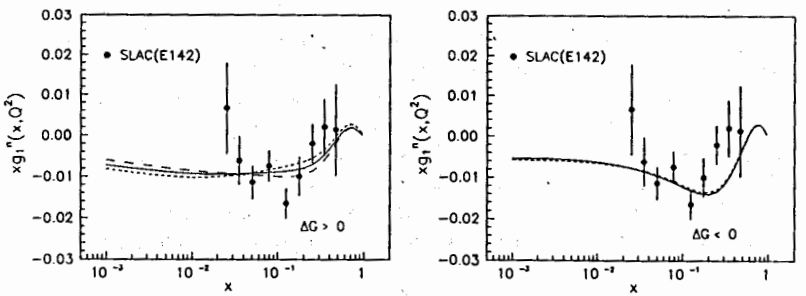

Figure 2. Deep-inelastic neutron structure function $xg_1^n(x,Q^2)$. Experimental data: $\bullet$ - [13]. Theoretical curves: (a) - $\Delta G > 0$ and (b) - $\Delta G < 0$ at $Q^2 = 10\ (GeV/c)^2$ - - -, ——, — — are obtained with parameters α_f, β_f of parton distributions taken from Tables (1,4), (2,5) and (3,6), respectively.

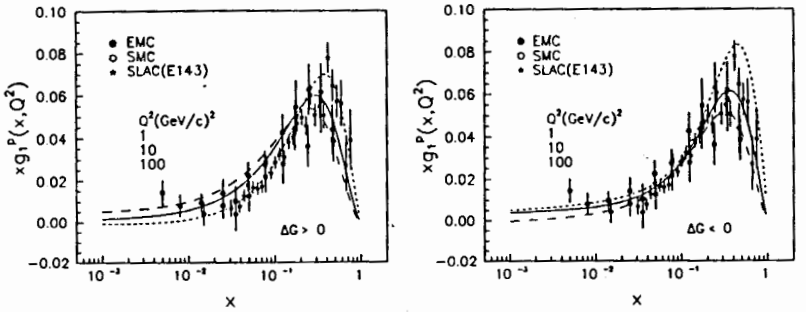

Figure 3. Deep-inelastic proton structure function $xg_1^p(x,Q^2)$. Experimental data: $\star$ - [1], $\bullet$ - [11], o - [14]. Theoretical curves: (a) - $\Delta G > 0$, (b) - $\Delta G < 0$ and - - - - 1 $(GeV/c)^2$, —— - 10 $(GeV/c)^2$, — — - 100 $(GeV/c)^2$. The parameters α_f, β_f of parton distributions are taken from Tables 2, 5.

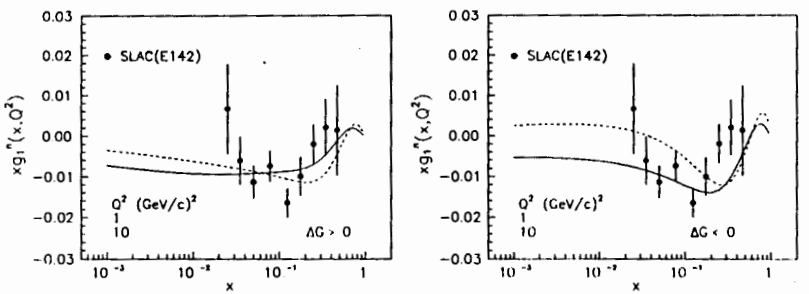

Figure 4. Deep-inelastic neutron xg_1^n structure function. Experimental data: $\bullet$ - [13]. Theoretical curves: (a) - $\Delta G > 0$, (b) - $\Delta G < 0$ and - - - - 1 $(GeV/c)^2$, —— - 10 $(GeV/c)^2$. The parameters α_f, β_f of parton distributions are taken from Tables 2, 5.

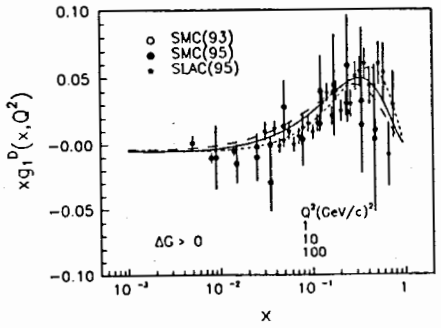

a)

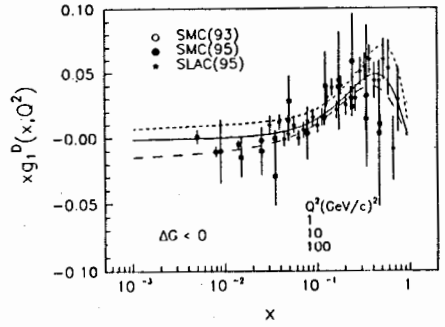

b)

Figure 5. Deep-inelastic deuteron xg_1^D structure function. Experimental data: $\star$ - [2], $\bullet$ - [3], $\circ$ - [12]. Theoretical curves: (a) - $\Delta G > 0$, (b) - $\Delta G < 0$ and - - - - - 1 $(GeV/c)^2$, ——— - 10 $(GeV/c)^2$, - - - - 100 $(GeV/c)^2$. The parameters α_f, β_f of parton distributions are taken from Tables 2, 5.

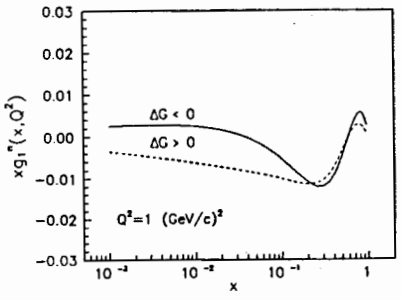

a)

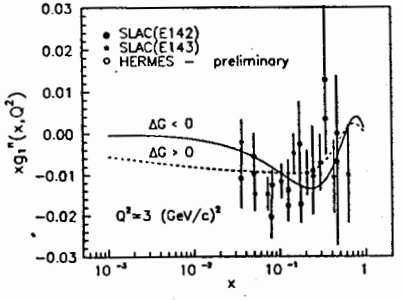

b)

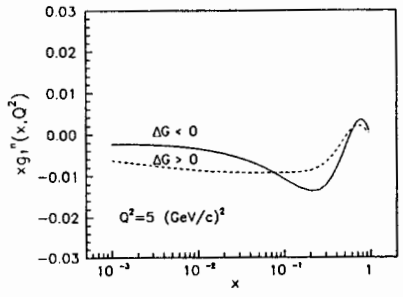

c)

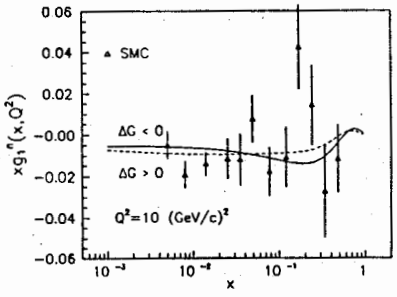

d)

Figure 6. Deep-inelastic neutron structure function $xg_1^n(x, Q^2)$. Experimental data: $\star$ - [2], $\triangle$ - [3], $\bullet$ - [13], $\circ$ - [15]. Theoretical curves: - - -·- $\Delta G > 0$, ——— - $\Delta G < 0$ at $Q^2 = 1, 3, 5, 10$ $(GeV/c)^2$. The parameters α_f, β_f of parton distributions are taken from Tables 2, 5.

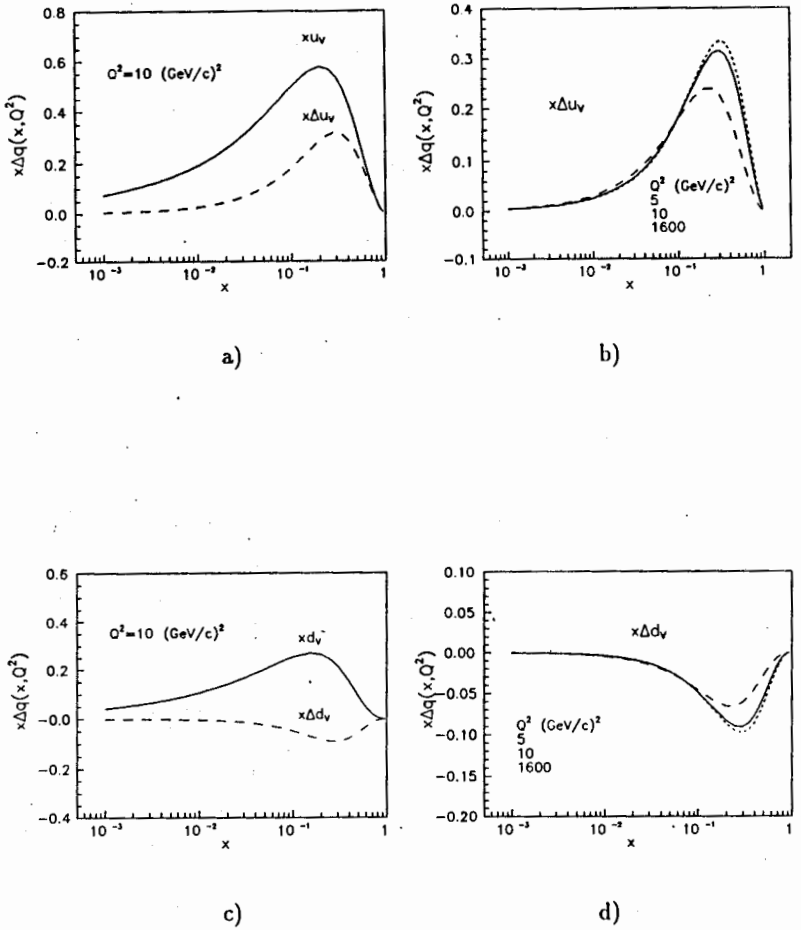

Figure 7. Dependence of the $x\Delta u_V$ and $x\Delta u_V$ valence parton distributions on x and Q^2 for positive sign of ΔG. Theoretical curves are obtained with parameters α_f, β_f taken from Table 2.

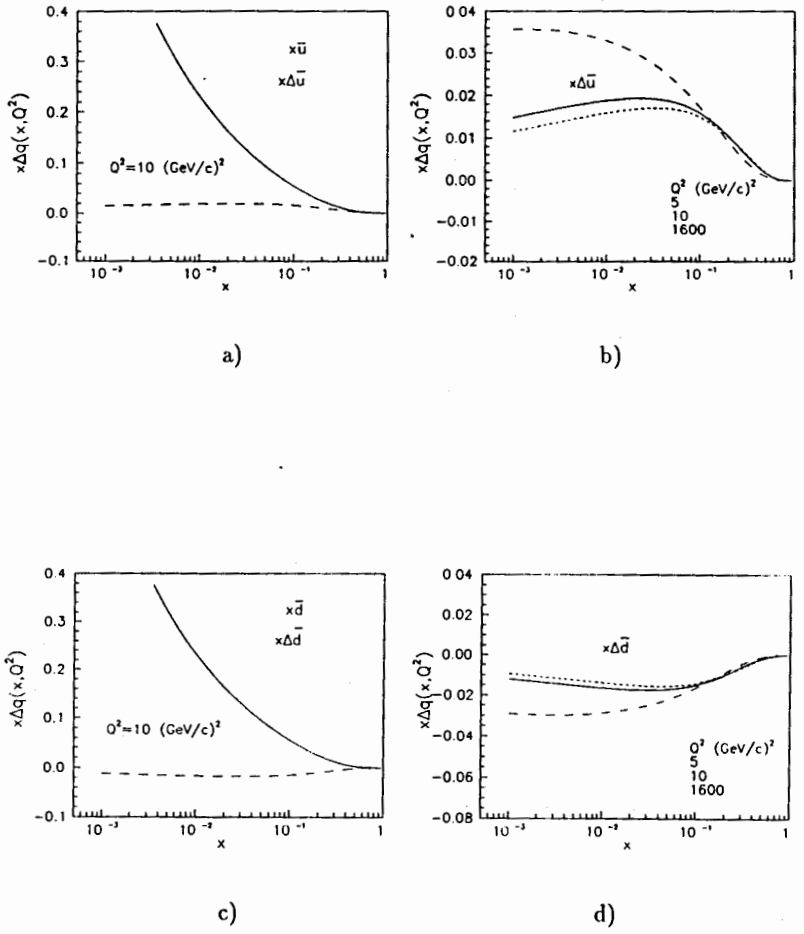

Figure 8. Dependence of the $x\Delta\bar{u}$ and $x\Delta\bar{d}$ valence parton distributions on x and Q^2 for positive sign of ΔG. Theoretical curves are obtained with parameters α_f, β_f taken from Table 2.

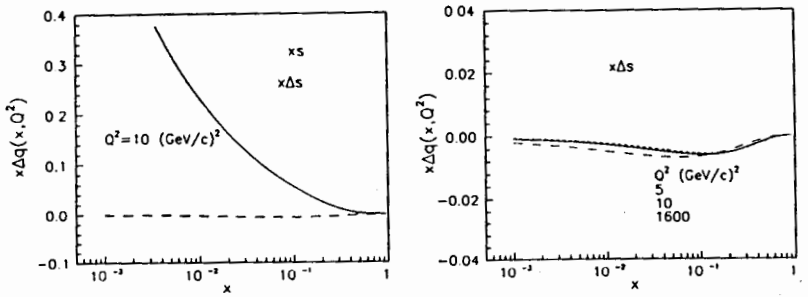

Figure 9. Dependence of the $x\Delta s$ and $x\Delta G$ parton distributions on x and Q^2 for positive sign of ΔG. Theoretical curves are obtained with parameters α_f, β_f taken from Table 2.

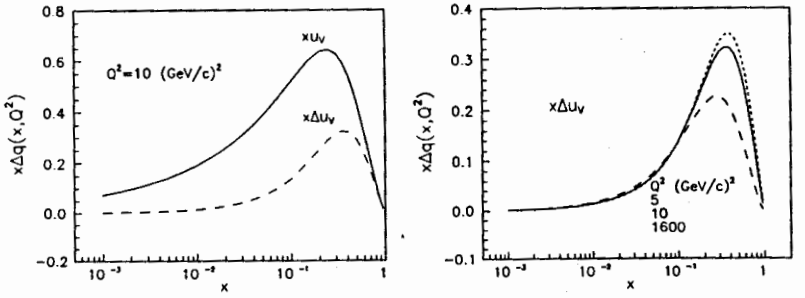

Figure 10. Dependence of the $x\Delta u_V$ and $x\Delta u_V$ valence parton distributions on x and Q^2 for negative sign of ΔG. Theoretical curves are obtained with parameters α_f, β_f taken from Table 5.

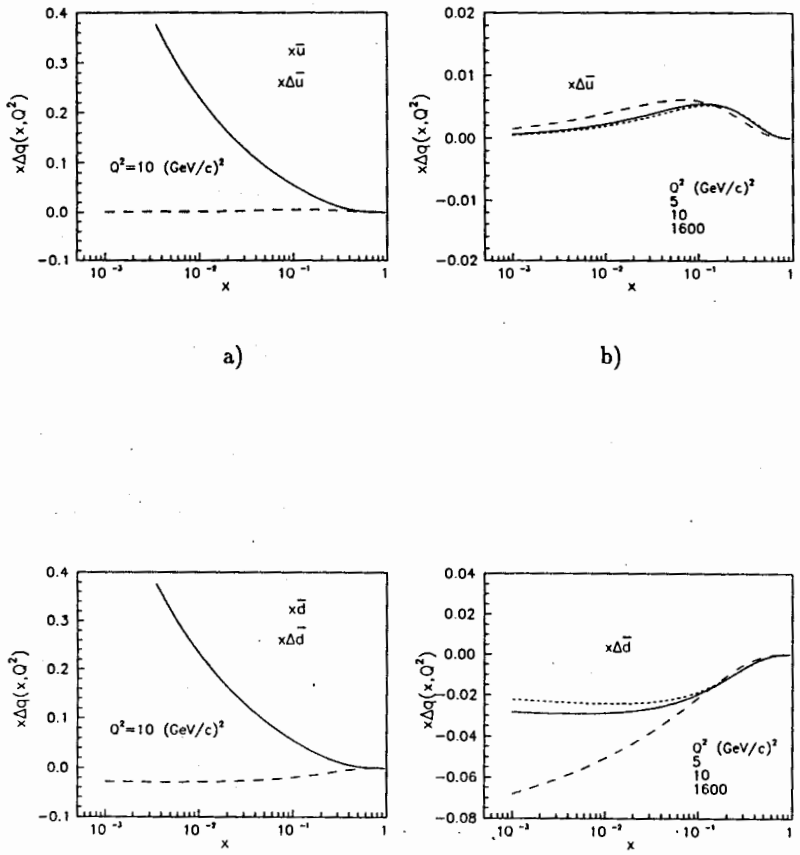

Figure 11. Dependence of the $x\Delta\bar{u}$ and $x\Delta\bar{d}$ valence parton distributions on x and Q^2 for negative sign of ΔG. Theoretical curves are obtained with parameters α_f, β_f taken from Table 5.

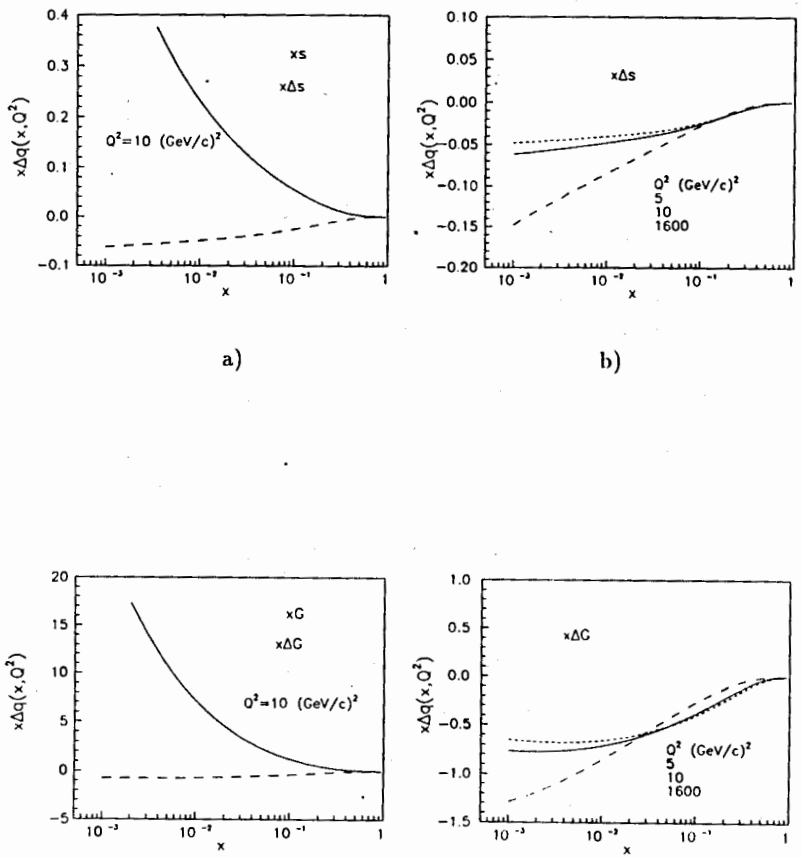

Figure 12. Dependence of the $x\Delta s$ and $x\Delta G$ parton distributions on x and Q^2 for negative sign of ΔG. Theoretical curves are obtained with parameters α_f, β_f taken from Table 5.

4 Conclusions

The method to construct spin-dependent parton distributions is considered. It bases on theoretical constraints (the shape, sign of Δq_f) and experimental data on quark contributions $\Delta u, \Delta d, \Delta s$ to proton spin. The new spin-dependent parton distributions $\Delta u_V, \Delta d_V, \Delta \bar{u}, \Delta \bar{d}, \Delta s, \Delta G$ are founded. The x- and Q^2-dependences of Δq_f for positive and negative ΔG are studied. The obtained results are compared with experimental data on structure functions g_1^p, g_1^D and g_1^n. It is found that g_1^n is sensitive to sign of ΔG and can be used to investigate the sign of gluon distribution in the range $x < 0.1$. The available experimental data on g_1^n give evidence that the sign of ΔG should be positive. The constructed parton distributions $\Delta u_V, \Delta d_V, \Delta \bar{u}, \Delta \bar{d}, \Delta s, \Delta G$ can be widely used to analyze both deep-inelastic (inclusive, semi-inclusive) and proton-proton interactions planed at RHIC, LHC and HERA.

5 Acknowledgement

The author would like to acknowledge A.V.Sidorov and W.-D.Nowak for a fruitful collaboration and helpful discussion and Yu.A.Panebratsev for his support of the work. This work was partially supported by Grants of Heisenberg-Landau Program for 1996 and of the Russian Foundation of Fundamental Research under No. 95-02-05061.

References

[1] K.Abe et al., *Phys. Rev. Lett.* **74** (1995) 346.

[2] K. Abe et al., *Phys. Rev. Lett.* **75** (1995) 25.

[3] D.Adams et al., *Phys. Lett.* **B357** (1995) 248.

[4] L.Whitlow et al., *Phys. Lett.* **B250** (1990) 193.

[5] R.L.Jaffe, *Phys. Lett.* **B365** (1996) 359.

[6] S.J. Brodsky, M. Burkardt, I.Schmidt, *Nucl.Phys.* **B273** (1995) 197.

[7] M. Gluck, E.Reya, W. Vogelsang, *Phys. Lett.* **B359** (1995) 210.

[8] T. Gehrmann, W.J.Stirling, *Z.Phys.* **C65** (1995) 461.

[9] J.F. Owens, *Phys. Lett.* **B266** (1991) 126.

[10] R.D.Ball, S. Forte, G.Ridolfi, Preprint CERN-TH/95-266, 1995.

[11] J.Ashman, et al., *Phys. Lett.* **B206** (1988) 210; *Nucl. Phys.* **B328** (1989) 1.

[12] B. Adeva et al., *Phys. Lett.* **B302** (1993) 533.

[13] P.L. Anthony et al., *Phys. Rev. Lett.* **71** (1993) 959.

[14] D.Adams et al., *Phys. Lett.* **B329** (1994) 399.

[15] M. Vetterli for the HERMES Collaboration, talk at the 'Workshop on Deep Inelastic Scattering', Rome, April 1996.

[16] G.'t Hooft, *Phys. Rev.* **D14** (1976) 3432.

[17] M.A.Shifman, A.I. Vainshtein, V.I. Zakharov, *Nucl.Phys.* **B163** (1980) 46.

[18] A.V. Efremov, O.V. Teryaev, Dubna report E2-88-287, 1988;
G. Altarelli, G.G. Ross, *Phys. Lett.* **B212** (1988) 391.

[19] J.Ellis, M.Karliner, Preprint CERN-TH. 7324/94, 1994.

[20] M.Gluck, E.Reya, A.Vogt, *Z.Phys.* **C48** (1990) 471.

Received by Publishing Department
on August 20, 1996.